9th Asia-Pacific Conference on Wind Engineering
Auckland, New Zealand
3-7 December 2017

Characteristics of local wind force and wind response of a building under short-rise-time gusts

T. Takeuchi[1], N. Takeuchi[1] , J. Maeda[2] and Y.C. Kim[3]

[1]Department of Architecture
Kobe University, Kobe, Hyogo 657-8501, Japan

[2]Faculty of Human-Environment Studies
Kyushu University, Fukuoka, Fukuoka 812-8581, Japan

[3]Department of Architecture
Tokyo Polytechnic University, Atsugi, Kanagawa 243-0297, Japan

Abstract

The characteristics of local wind force of a square prism under a short-rise-time gust were investigated using a CFD simulation with an LES model, and the wind response of the prism under a short-rise-time gust was calculated. It was confirmed that the overshoot phenomena of local wind force occurred on the windward and leeward faces of the square prism subjected to a short-rise-time gust, as well as the wind pressure. It was found that the overshoot phenomenon of local wind force was more remarkable in the case that the prism was higher. And we confirmed the overshoot phenomenon of response displacement for the model subjected to the short-rise-time gust, and the maximum value of the displacement obtained by the dynamic analysis was larger than that obtained by the static analysis.

Introduction

Several studies [1-7] indicate that an overshoot phenomenon bringing a much larger wind force than in a steady flow occurs on a body under a gusty wind with a very short rise time. Taneda [1] investigated unsteady lift acting on an elliptic cylinder rapidly started at an angle of attack using a water tank test and reported that a remarkably big lift appeared just after starting. Sarpkaya [2] showed that the drag of a body increased by about 25 percent during the growth of the first pair of vortices as compared to a steady flow, using an impulsive flow test over circular cylinders in a vertical water tunnel, adding some results of potential flow analyses around the circular cylinders. Nomura et al. [3] computed unsteady drag acting on a square cylinder under a sudden change of flow speed and reported that the drag component proportional to flow acceleration played quite an important role in the total unsteady drag when the flow speed was relatively low. Matsumoto et al. [4] measured transient drag on a two-dimensional cylindrical model under a suddenly-changing wind speed using a wind tunnel test with a working section of 200mm by 200mm square, and reported an overshoot phenomenon in which the drag increased by approximately 20% compared to the force in a steady flow. Noda et al. [5] measured transient drag forces acting on a square prism with several angles of attack under a step-function-like rapidly-changing wind speed in an experiment using towing tank equipment. The present authors investigated the unsteady wind force and the unsteady wind pressure on a body under a short-rise-time gust using a specially-equipped wind tunnel, which can generate gusts with a rise time of 0.2 to 5 seconds by controlling the rotation speed of the blade rows [6-7]. And we investigated the effects of wind direction on unsteady wind pressure on the flat roof body and the gable roof body under a short-rise-time gust using the gust wind tunnel and a CFD simulation, and reported that the overshoot phenomenon was strongly affected by the unsteady vortices generated at the windward edge of the flat roof face and the verge and ridge on the gable roof face [8]. However, the characteristics of local wind force and wind response of a building under a short-rise-time gust has not been well clarified. In this study, the characteristics of local wind force acting on a square prism under a short-rise-time gust were investigated using a CFD simulation with an LES model. And then, the wind response of the prism subjected to a short-rise-time gust was calculated.

General specifications of CFD simulation

The flow around a square prism subjected to a step-function-like gust was simulated by CFD software using an LES model, as shown in Figure 1. An incompressible flow was assumed and the differential equations were discretized by the finite volume method. The upwind difference scheme was applied to the

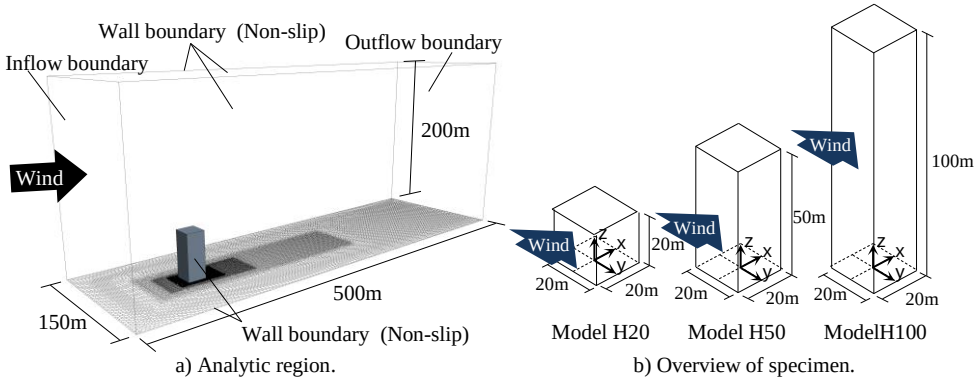

a) Analytic region. b) Overview of specimen.

Figure 1. Analytic region and overview of specimen.

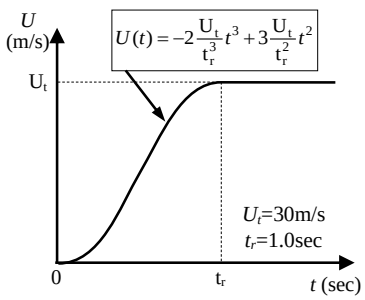

Figure 2. Inflow wind velocity.

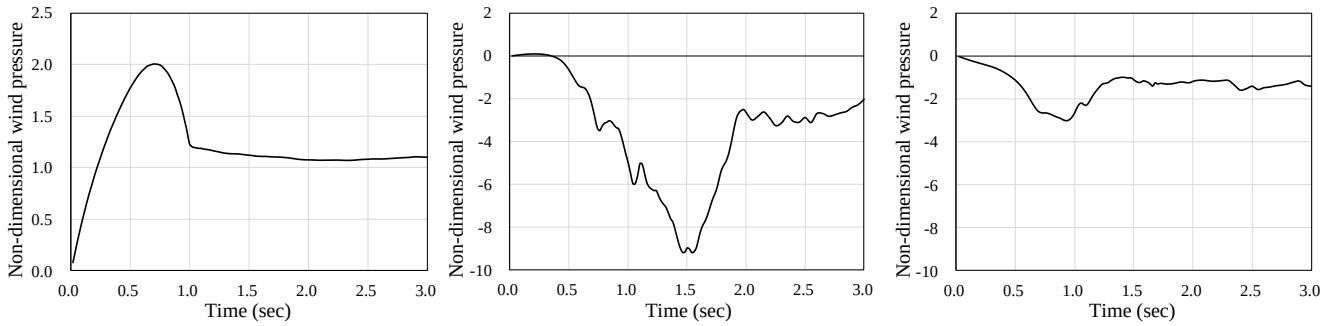

a) At a point (y=2, z=25) on the windward wall face.

b) At a point (x=-9, z=48) on the side wall face.

c) At a point (y=9, z=48) on the leeward wall face.

Figure 3. Time evolutions of wind pressure (model H50).

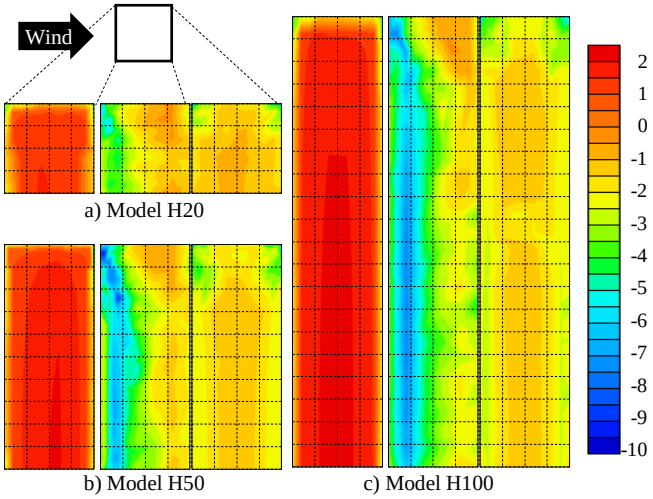

Figure 4. Distributions of the overshoot wind pressure coefficients.

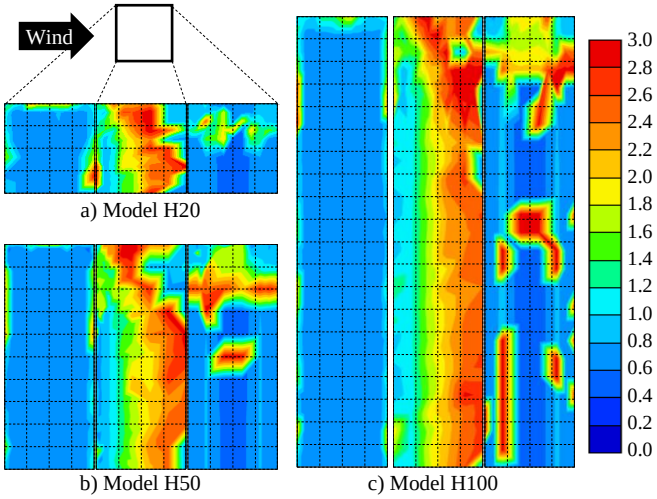

Figure 5. Distributions of the time when the pressure reached a peak.

convective term. The central difference scheme was applied to the viscous term. The pressure and velocities were coupled by means of the Pressure Implicit with Splitting of Operators (PISO) method. The LES/Smagorinsky model was used for the turbulence model. The analytic region was nested, and the maximum size of the cells near the square prism was 0.2m. The boundary conditions of the model were set up as shown in Figure 1. We modeled the inflow wind velocity on the short-rise-time wind velocity measured in the wind tunnel tests, as shown in Figure 2. This paper presents the simulated results using the inflow wind velocity when it varied from calm to 30m/s in a rise time of 1.0sec.

The specimens were square prisms, as shown in Figure 1b. The width of the prisms was 20m. The prisms were 20m, 50m and 100m high, and referred to as “model H20”, “model H50” and “model H100”, respectively. The wind direction directly faced the wall face of the prism. The wind pressure was output at many points on the surface of the prism. The effect of a rapid change of static pressure was eliminated in the same way as in the reference [8].

Characteristics of unsteady wind pressure

Figure 3 shows the time evolutions of pressure at 3 points on the windward, side and leeward faces of model H50. The vertical axis of a graph in this figure shows the wind pressure divided by velocity pressure under a steady flow. We confirmed the overshoot phenomena of wind pressure, which reached much larger values than the steady values on each point. The peak value at the point on the windward face was positive, and the peak values at the points on the side and leeward faces were negative. Figure 4 shows the distributions of the overshoot wind pressure coefficients on the surface of each model. The overshoot wind pressure coefficient was defined by dividing the peak value by velocity pressure under a steady flow.

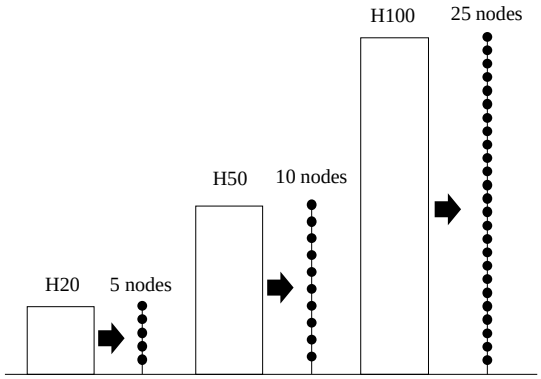

Figure 6. Conversion to a mass-spring model.

On the windward face, the overshoot wind pressure coefficient was almost constant around the center of the face, and the value decreased toward the end of the face. On the side faces of models H50 and H100, the overshoot wind pressure coefficient was high near the upper-windward corner. However, on the middle or lower part of the prism, the overshoot wind pressure coefficient was high at the region located 5~10m leeward from the windward edge of the side face. On the leeward face, the overshoot wind pressure coefficient was high near the upper corners.

Figure 5 shows the distributions of the time when the pressure reached a peak. On the windward face, the wind pressure on most points reached a peak at approximately 0.7sec. On the side face, the peak time changed with the distance from the windward end. The reason for this might be that the unsteady vortex which caused the overshoot phenomenon of wind pressure was generated from the windward end of the side face, and moved backward with the time. On the leeward face, the peak time on some spots was late, but the peak time on the other part was almost constant

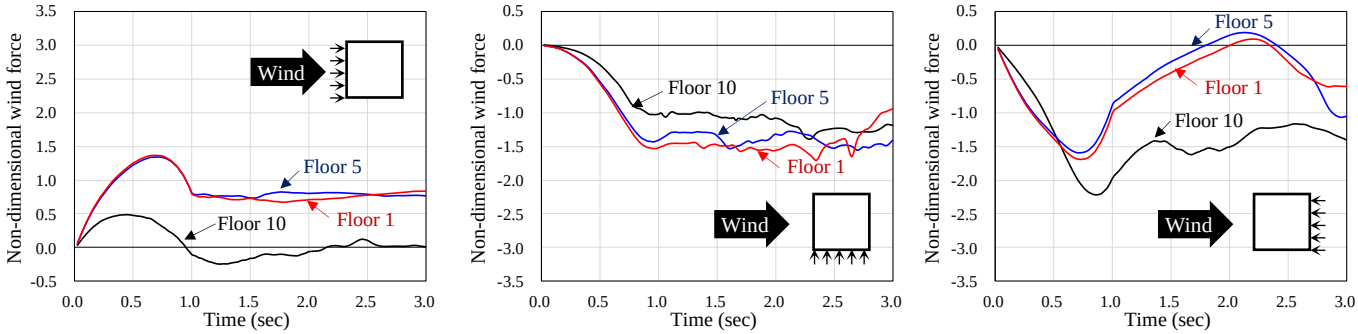

a) On the windward wall face b) On the side wall face c) On the leeward wall face

Figure 7. Time evolutions of local wind force acting on wall faces of Model H50.

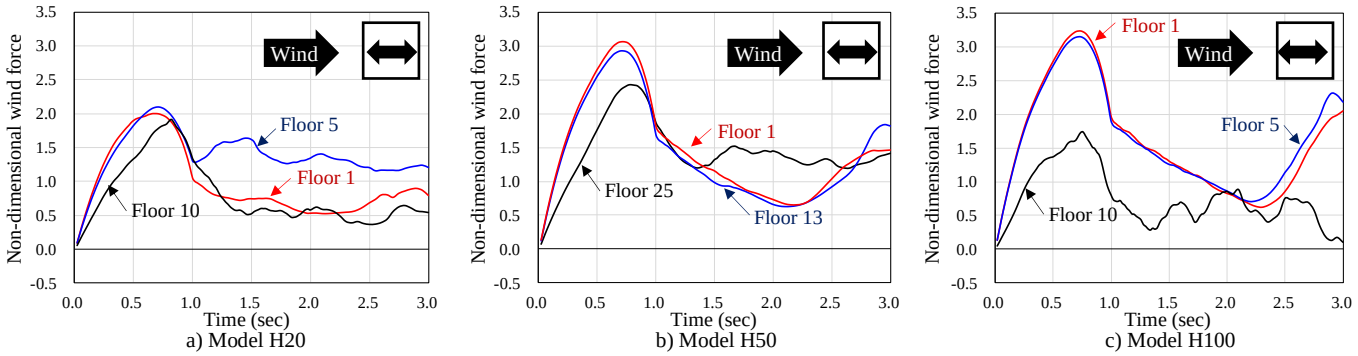

a) Model H20 b) Model H50 c) Model H100

Figure 8. Time evolutions of local along-wind force.

Characteristics of unsteady local wind force

Models H20, H50 and H100 w ere conversed to mass-spring models of 5 nodes, 10 nodes and 25 nodes, respectively, as shown in Figure 6. And the local wind force at each story of these models was obtained by summing the output pressure multiplied by its reference area. Figure 7 shows the time evolutions of the local wind force at the first, middle and uppermost stories acting on the windward, side and leeward faces of model H50. The vertical axis of a graph in this figure shows the local wind force divided by velocity pressure under a steady flow. The overshoot phenomena of local wind force on the windward and leeward faces were confirmed as well as the wind pressure. On the side face, the overshoot phenomenon of local wind force scarcely occurred, while the overshoot phenomenon of wind pressure was considerably large. The reason for this seems to be that the time when the unsteady wind pressure reached a peak differed with the location of the output point on the side face, as show in Figure 5. But, it was expected that the overshoot phenomenon of local wind force on the side face affected by the wind direction . Figure 8 shows the time evolutions of the local along-wind forces acting on model H50 obtained by adding the wind pressure on the windward and leeward faces. Figure 9 shows the distributions of maximum value of non-dimensional local along-wind force. It was found that the overshoot phenomenon of local wind force was more remarkable when the building subjected to the gust was higher.

Wind Response Analysis

The wind response of the prism receiving the local along-wind forces obtained in the previous session was calculated. The prisms were modeled as a group of lumped point masses interconnected with shear springs without mass. The distribution of the stiffness of springs were controlled to adjust the shape of the primary mode to a linear shape. And the value of the stiffness was determined by the primary natural period. The weight of each mass was 480ton. The damping ratio of each mode of the model was set at 2%. The displacement of the nodes was calculated using Newmark-beta method at 0.01sec intervals. The primary natural period of the models, T_1, was set as shown in Table 1.

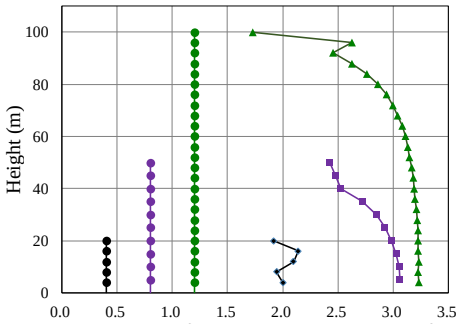

Figure 9. Distributions of maximum value of non-dimensional local along-wind force.

	0.015H	0.02H	0.025H	0.03H	0.04H
Model H20	0.03	0.04	0.05	0.06	0.08
Model H50	0.75	1	1.25	1.5	2
Model H100	1.5	2	2.5	3	4

Table 1. Setting values of the primary natural period of models.

Figure 10 shows the time evolutions of displacement of the top nodes of model H20 of T_1 = 0.4sec, model H50 of T_1 = 0.75sec and 1.5sec, and model H100 of T_1 = 1.5sec. The blue line in this figure show the response calculated by a static analysis. We confirmed that the overshoot phenomenon of displacement occurred for the model subjected to the short-rise-time gust. And it was found that the maximum value of the displacement obtained by the dynamic analysis was larger than that obtained by the static analysis. The dynamic effect showed a tendency to increase with the primary natural period. Figure 11 shows the distributions of maximum values of the relative story displacement. In the cases that the primary natural period was short, the relative story displacement at the lower floor was larger than that at the upper floor. On the other hand, in the cases that the primary natural period was longer, the relative story displacement at the upper floor was larger. The reason for this was that the effect of the secondary mode of the model to the response increased with the primary natural period. It would appear that the response of a

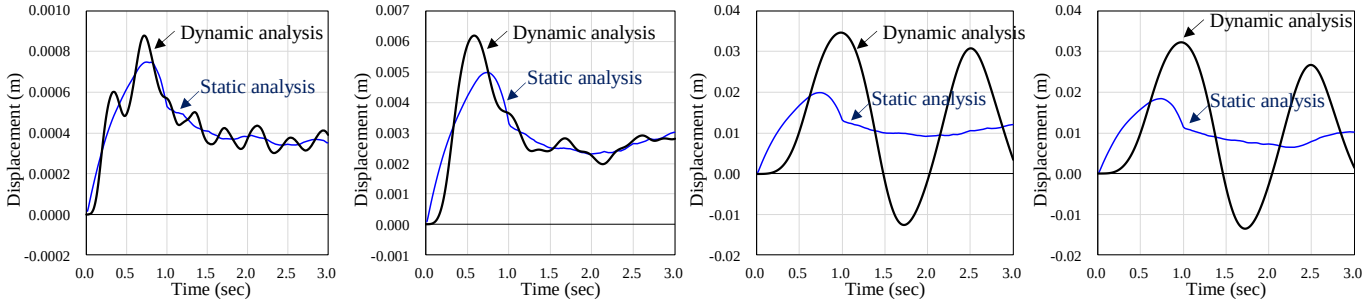

a) Model H20, T_1 = 0.4sec b) Model H50, T_1 = 0.75sec c) Model H50, T_1 = 1.5sec d) Model H100, T_1 = 1.5sec

Figure 10. Time evolutions of displacement of the top node.

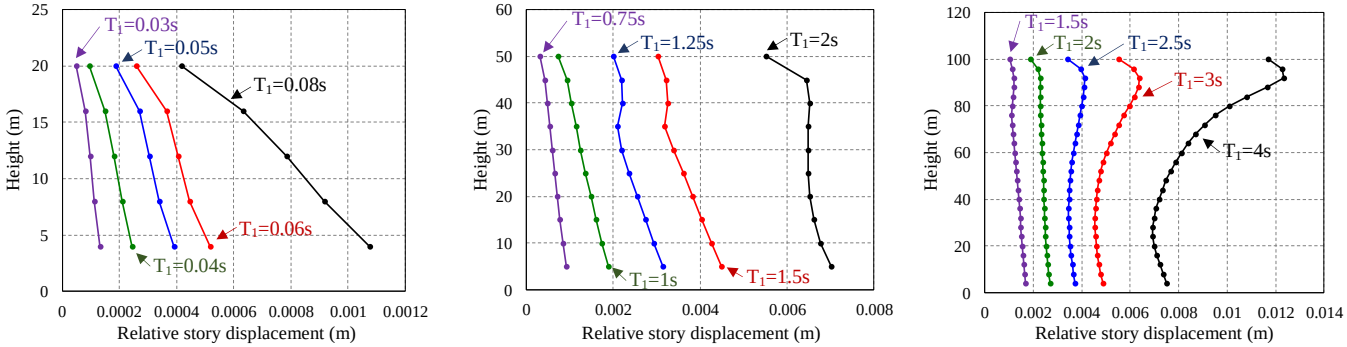

a) Model H20 b) Model H50 c) Model H100

Figure 11. Distributions of maximum values of the relative story displacement.

building subjected to a short-rise-time gust affected by the ratio of the natural period of the building to the rise time of gust.

Conclusions

- It was confirmed that the overshoot phenomena of local wind force occurred on the windward and leeward faces of a square prism subjected to a short-rise-time gust, as well as the wind pressure. It was found that the overshoot phenomenon of local wind force was more remarkable in the case that the prism was higher.
- On the side face, the overshoot phenomenon of local wind force scarcely occurred, while the overshoot phenomenon of wind pressure was considerably large. The reason for this seems to be that the time when the unsteady wind pressure reached a peak differed with the location of the output point on the side face.
- It was confirmed that the overshoot phenomenon of response displacement occurred for the model subjected to the short-rise-time gust, and the maximum value of the displacement obtained by the dynamic analysis was larger than that obtained by the static analysis.

Acknowledgements

This study was supported by Grant-in-Aid for Scientific Research (B), No.26282112, Grant-in-Aid for Young Scientists (B), No.15K18155, and Grant-in-Aid for Scientific Research (C), No. 17K06643, Japan Society for the Promotion of Science. This study has been partially supported Year 2016 Joint Usage/Research Program through Wind Engineering Research Center in Tokyo Polytechnic University..

References

[1] Taneda, S., The Development of the Lift of an Impulsively Started Elliptic Cylinder at Incidence, Journal of the Physical Society of Japan, Vol. 33, No. 6, pp.1706-1711, 1972.

[2] Sarpkaya, T., Separated Flow about Lifting Bodies and Impulsive Flow about Cylinders, AIAA Journal, Vol. 4, No. 3, 414-420, 1966.

[3] Matsumoto, M., Shimamura, M., Maeda, T., Shirato, H., Yagi, T., Hori, K., Kawashima, Y. and Hashimoto, M., Drag forces on 2-D cylinders due to sudden increase of wind velocity, 12th International Conference on Wind Engineering, Preprints-Vol.2, pp.1727-1734, 2007.

[4] Nomura, T., Kitamura, N. and Kitagawa, T., Characteristics of unsteady drag on a square cylinder under sudden change of wind speed, Proceedings of Computational Wind Engineering, pp.3-6, 2000.

[5] Noda, M., Hisanobu, S., Waki, T. and Nagao, F., Overshoot coefficient of transient drag forces on square prism in quick change of wind speed, Proceedings of 22nd National Symposium on Wind Engineering, Tokyo, 133-138, 2012 (in Japanese).

[6] Takeuchi, T. and Maeda, J., Unsteady wind force on an elliptic cylinder subjected to a short-rise-time gust from steady flow, Journal of Wind Engineering and Industrial Aerodynamics, Vol.122, 138-145, 2013.

[7] Takeuchi, T., Maeda, J., Otsubo, K. and Tomokiyo E., Unsteady wind pressure on a body under short-rise-time gust, Journal of Structural and Construction Engineering: Transactions of AIJ 697, 357-366, 2014 (in Japanese).

[8] Takeuchi, T., Maeda, J., Kawakami R. and Takeuchi N., Effects of wind direction and roof shape on unsteady wind pressure on a low rise building under a short-rise-time gust, Proceedings of 8th International Colloquium on Bluff Body Aerodynamics and Applications, 9pages, 2016.6.